Diffraction cancellation over multiple wavelengths in photorefractive dipolar glasses

J. Parravicini,[1,2] F. Di Mei,[3] C. Conti,[4] A. J. Agranat,[5] and E. DelRe,[1,2,*]

[1]*Department of Electrical and Information Engineering, University of L'Aquila, 67100 L'Aquila, Italy*
[2]*IPCF-CNR, University of Rome "La Sapienza", 00185 Rome, Italy*
[3]*Department of Physics, University of Rome "La Sapienza", 00185 Rome, Italy*
[4]*Department of Molecular Medicine and ISC-CNR, University of Rome "La Sapienza", 00185 Rome, Italy*
[5]*Applied Physics Department, Hebrew University of Jerusalem, 91904 Israel*
[*]*eugenio.delre@univaq.it*

Abstract: We report the simultaneous diffraction cancellation for beams of different wavelengths in out-of-equilibrium dipolar glass. The effect is supported by the photorefractive diffusive nonlinearity and scale-free optics, and can find application in imaging and microscopy.

OCIS codes: (190.0190) Nonlinear optics; (050.1940) Diffraction; (160.2260) Ferroelectrics; (160.5320) Photorefractive materials.

References and links

1. E. DelRe, E. Spinozzi, A. J. Agranat, and C. Conti, "Scale-free optics and diffractionless waves in nanodisordered ferroelectrics," Nat. Photon. **5,** 39-42 (2011).
2. C. Conti, A. J. Agranat, and E. DelRe, "Subwavelength optical spatial solitons and three-dimensional localization in disordered ferroelectrics: towards metamaterials of nonlinear origin," Phys. Rev. A **84**, 043809 (2011).
3. D. Marcuse, *Theory of Dielectric Optical Waveguides* (Academic Press, New York, 1974).
4. A. Yariv, *Quantum Electronics*, 3rd Edition (Wiley, New York, 1989).
5. S. Trillo and W. Torruellas (eds.), *Spatial solitons* (Springer-Verlag, Berlin, 2001).
6. D. Kip, C. Anastassiou, E. Eugenieva, D. Christodoulides, and M. Segev, "Transmission of images through highly nonlinear media by gradient-index lenses formed by incoherent solitons," Opt. Lett. **26,** 524-526 (2001).
7. J. K. Yang, P. Zhang, M. Yoshihara, Y. Hu, and Z. G. Chen, "Image transmission using stable solitons of arbitrary shapes in photonic lattices ," Opt. Lett. **36**, 772-774 (2011)
8. O. Firstenberg, P. London, M. Shuker, A .Ron, and N. Davidson, "Elimination, reversal and directional bias of optical diffraction," Nat. Phys. **5**, 665-668 (2009)
9. D. V. Dylov and J. W. Fleischer, "Nonlinear self-filtering of noisy images via dynamical stochastic resonance," Nat. Photon. **4**, 323-328 (2010)
10. D .B. Murphy, *Fundamentals of light microscopy and electronic imaging* (Wiley, New York, 2001)
11. B. Crosignani, E. DelRe, P. Di Porto, and A. Degasperis, "Self-focusing and self-trapping in unbiased centrosymmetric photorefractive media," Opt. Lett. **23**, 912-914 (1998)
12. B. Crosignani, A. Degasperis, E. DelRe, P. Di Porto, and A. J. Agranat, "Nonlinear optical diffraction effects and solitons due to anisotropic charge-diffusion-based self-interaction," Phys. Rev. Lett. **82**, 1664-1667 (1999)
13. E. DelRe, B. Crosignani, and P. Di Porto, "Photorefractive Solitons and Their Underlying Nonlocal Physics ," Prog. Optics **53**, 153-200 (2009)
14. G. Samara, "The relaxational properties of compositionally disordered ABO_3 perovskites," J. Phys.: Condens. Matter **15**, R367-R411 (2003)
15. A. A. Bokov, and Z. -G. Ye, "Recent progress in relaxor ferroelectrics with perovskite structure," J. Mater. Sci **41**, 31-52 (2006)

#154747 - $15.00 USD Received 16 Sep 2011; revised 13 Oct 2011; accepted 14 Oct 2011; published 10 Nov 2011

16. P. Ben Ishai, A. J. Agranat, and Y. Feldman, "Confinement kinetics in a KTN : Cu crystal: Experiment and theory," Phys. Rev. B **73**, 104104 (2006)

1. Introduction

Diffraction is a fundamental limit to optical imaging, microscopy, and information transfer. Recent experiments [1] and theoretical arguments [2] have shown that diffraction can be cancelled in a system with an intensity-independent nonlinear response that acts in the form of an anti-diffraction. Diffraction cancellation implies that beams do not spread because diffraction is absent, and not simply because it is compensated by an index of refraction pattern, such as in a waveguide [3, 4], or because of a nonlinear index change, such as in solitons [5]. In both these cases, diffraction compensation introduces limits on the non-spreading waves, such as the optical modal structure of the waveguide and the soliton existence conditions, that require specific solutions to allow effective image transfer [6, 7]. In diffraction cancellation, these strict laws are absent and the optical propagation occurs without any limit associated to the optical wavelength, a condition termed scale-free optics [1] that is also related to recent findings in slow-light experiments [8].

A basic application of scale-free optics is in imaging or in microscopy, where nonlinearity is known to play a fundamental role [9]. However, in these systems the optical field typically has a large spectral content. In fluorescence microscopy, the optical image to be collected and transferred through the optical system is simply multi-colored [10]. To date, all experiments into diffraction cancellation and scale-free optics have been limited to a single optical wavelength. The question lies open if and how diffraction cancellation can be achieve for colored images, that is, for optical fields composed of different wavelengths.

In this Letter we report the simultaneous cancellation of diffraction for a green $\lambda_1 = 532$ nm and a red $\lambda_2 = 633$ nm laser beam of same size and intensity. The phenomenon is supported by the scale-free diffusive nonlinearity [11–13] observed in a disordered photorefractive ferroelectric crystal [14–16], and emerges through the enhanced electro-optic response of polar nanoregions (PNR) that form when the crystal is supercooled close to its room temperature Curie point T_C [1, 2].

2. Model

In a dipolar glass, PNR form a liquid-like medium that has the remarkable property of having a scalar electro-optic response [1]

$$\Delta n_{ij} = -\frac{1}{2} n_0^3 \delta_{ij} g \mathbf{P} \cdot \mathbf{P} \tag{1}$$

where Δn_{ij} is the electro-optic tensor, n_0 is the crystal unperturbed index of refraction, g the effective quadratic electro-optic coefficient, δ_{ij} the Kronecker symbol, and $\mathbf{P}$ the low frequency polarization of the glass. When the dipolar glass is photorefractive, photoexcited charges diffuse and give rise to the steady-state electric field [1]

$$\mathbf{E}_d = -\frac{k_B T}{q} \frac{\nabla I}{I} \tag{2}$$

where k_B is the Boltzmann constant, T the crystal temperature, q the charge of the diffusing ions, and I is the local optical intensity. When the dipolar glass is brought far from equilibrium the PNR become highly polarizable and the result is a giant electro-optic response: low frequency polarization $\mathbf{P} = \varepsilon_0 \chi_{PNR} \mathbf{E}_d$ is dominated by the PNR susceptibility $\chi_{PNR} \gg \chi$, where χ is the equilibrium low-frequency susceptibility, and χ_{PNR} depends strongly on the previous thermal history of the nanodisordered ferroelectric. Inserting Eq. (1) and Eq. (2) into the

#154747 - $15.00 USD Received 16 Sep 2011; revised 13 Oct 2011; accepted 14 Oct 2011; published 10 Nov 2011

parabolic equation that describes the scalar paraxial propagation of a single linear polarization component of the slowly-varying optical field A ($|A|^2 = I$ is the optical intensity)

$$2ik\frac{\partial A}{\partial z} + \nabla_{\perp}^2 A + \frac{2k^2}{n_0}\Delta n A = 0, \tag{3}$$

we obtain [1, 2]

$$2ik\frac{\partial A}{\partial z} + \nabla_{\perp}^2 A - \frac{L^2}{4\lambda^2}\frac{(\partial_x I)^2 + (\partial_y I)^2}{I^2}A = 0, \tag{4}$$

where

$$L = 4\pi n_0^2 \varepsilon_0 \sqrt{g}\chi_{PNR}(K_B T/q). \tag{5}$$

Here L is the characteristic length scale introduced by the diffusive response, $k = 2\pi n_0/\lambda$, and $\Delta n = \Delta n_{xx}$, assuming x is the direction of the linear polarization of the beam. In general, in Eq. (3) the Δn does not introduce a spatial scale. Examples of this are the guiding index of refraction patterns of optical waveguides, or the self-focusing responses of Kerr-like media. In turn, the specific form of the nonlinearity that emerges from Eq. (1) and Eq. (2) introduces a new spatial scale L (see Eq. (5)), and this profoundly transforms the transverse dynamics of the propagation. In the second and third terms of Eq. (4), i.e., in those terms that drive the transverse dynamics of the beam, λ only appears normalized to L. If we neglect the weak dispersion in L due to the material dispersion, that is, the dependence of n_0 and χ_{PNR} on λ, L is fixed through the supercooling of the dipolar glass and forms a threshold value for the optical spectrum [1, 2]. Spectral components with $\lambda = L$ will form Gaussian beams that do not diffract; those with $\lambda < L$ will also form beams that have a cancelled diffraction, but with a shape that is slowly morphed from the original Gaussian beam typical of laser modes, to a more exotic diamond-like shape that intervenes for $\lambda \ll L$ [1, 2]. Instead, $\lambda > L$ components will diffract. Accordingly, diffraction cancellation supported by scale-free optics should hold for all beams with $\lambda \leq L$, to the point that fixing a large enough L extends this conditions to a large portion of the visible spectrum, and all these wavelengths can be subject to scale-free propagation simultaneously.

3. Single-wavelength experiments

We carry out our experiments in Lithium-enriched potassium-lithium-tantalate niobate (KTN:Li), a crystal with complex dielectric behavior that has both relaxor-like response and strong photorefractive response induced by Cu impurities [1]. The crystal temperature is established by a current-controlled Peltier-junction, and two optical TEM_{00} beams, respectively from a doubled Nd-Yagg laser ($\lambda_1 = 532$ nm) and a He-Ne laser ($\lambda_2 = 633$ nm) are first expanded an focused down onto the input facet of the crystal. The two beams have independent optical paths and are recombined through a standard beam-splitter right before the crystal, so that both their size, intensity, polarization, and focusing can be fixed separately. In our basic experiment, we fix both beams to an approximately circular intensity distribution of equal intensity Full-Width-at-Half-Maximum (FWHM) $\Delta x \simeq \Delta y \simeq 12\ \mu$m, and equal peak intensity of $I_{p1} \simeq I_{p2} \simeq 50\ \mathrm{W/cm^2}$, copropagating in parallel and with the same x linear polarization.

We first proceed to determine the conditions of supercooling that lead to scale-free propagation for the two wavelength beams separately.

In Fig. 1 we demonstrate that for a cooling rate of $\alpha_1 \simeq 0.11^{\circ}\mathrm{C/s}$ (see the thermal cooling process in Fig. 1(d)) we observe the output intensity distribution to pass from the spread out shape caused by diffraction ($\Delta x \simeq \Delta y \simeq 30\mu$m, Fig. 1(a,b)) to the non-diffracting case (Fig. 1(c)), where the input beam size is held throughout the $L_z = 3$mm propagation in the sample (this being the threshold value of χ_{PNR} associated to the value of α_1 for which $L = L_1 = \lambda_1$).

#154747 - $15.00 USD Received 16 Sep 2011; revised 13 Oct 2011; accepted 14 Oct 2011; published 10 Nov 2011

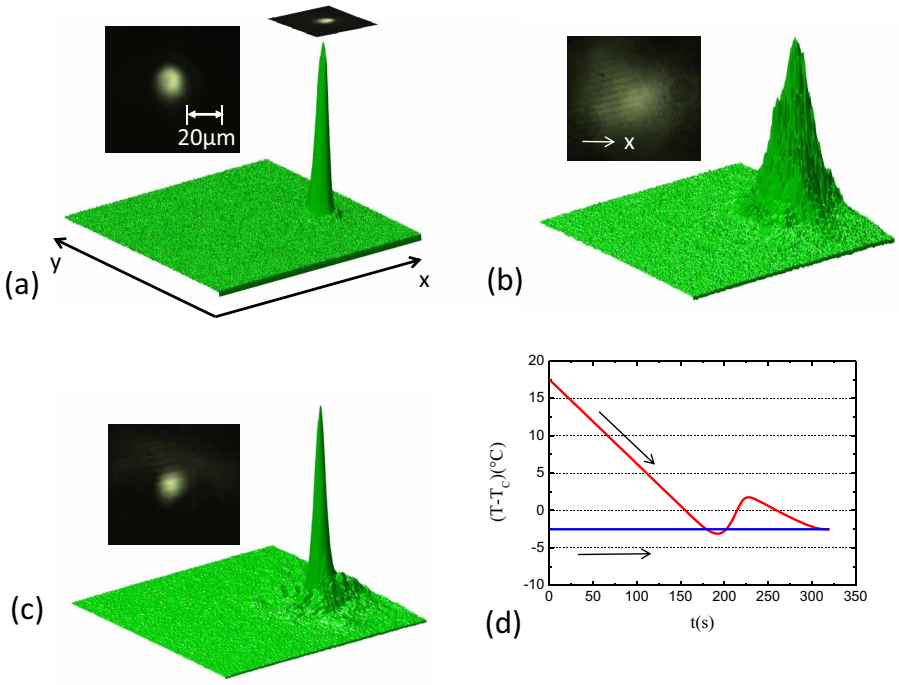

Fig. 1. Green ($\lambda = \lambda_1$) scale-free propagation and supercooling process. (a) Input intensity distribution, (b) output intensity distribution with no supercooling, (c) with the threshold supercooling α_1. (d) Comparison between the supercooling (red line) and no supercooling (blue line) glass preparation ($T_C \simeq 14.5°$C in our sample). The final dip in the temperature trajectory for the supercooling case is the standard overshooting of the temperature control circuit.

Analogoulsy, in Fig. 2 we determine that scale-free propagation is observed for the red beam at $\alpha_2 \simeq 0.13°\text{C/s}$ (see Fig. 2(d)), for which hence $L = L_2 = \lambda_2$. We note that the threshold cooling rates for the dipolar glass scale $\alpha_1/\alpha_2 \simeq 0.84 \simeq \lambda_1/\lambda_2$, as expected from the scale-free model, being that $\chi_{PNR} \propto \alpha$ (and $L \propto \chi_{PNR}$, see Eq. (5)).

4. Dual-wavelength experiments

We next pass to detecting wavelength-insensitive propagation by using a cooling rate that attenuates diffraction sensibly for both beams, and shine simultaneously the two beams at a transverse distance of 90 μm (so as to not undergo interaction) in the horizontal direction. We select $\alpha = 0.13°\text{C/s}$, so that $L = \lambda_2$ is the critical value for scale-free optics. In these conditions we expect the λ_1 beam to be above the scale-free propagation threshold $L > \lambda_1$. What we observe is reported in Fig. 3. Remarkably, as shown in Fig. 3(a), the two beams propagate in the very same manner, suffering no chromatic effects, even though one is green and the other is red, in accordance with what expected from Eq. (4). Interestingly, the same conditions of scale-free propagation are observed for a wide range of peak intensities, also for $I_{p1} \neq I_{p2}$, as expected from the intensity-independence of the scale-free model (see Fig. 4).

We note that to carry out the double wavelength experiments we have adopted techniques to

#154747 - $15.00 USD Received 16 Sep 2011; revised 13 Oct 2011; accepted 14 Oct 2011; published 10 Nov 2011

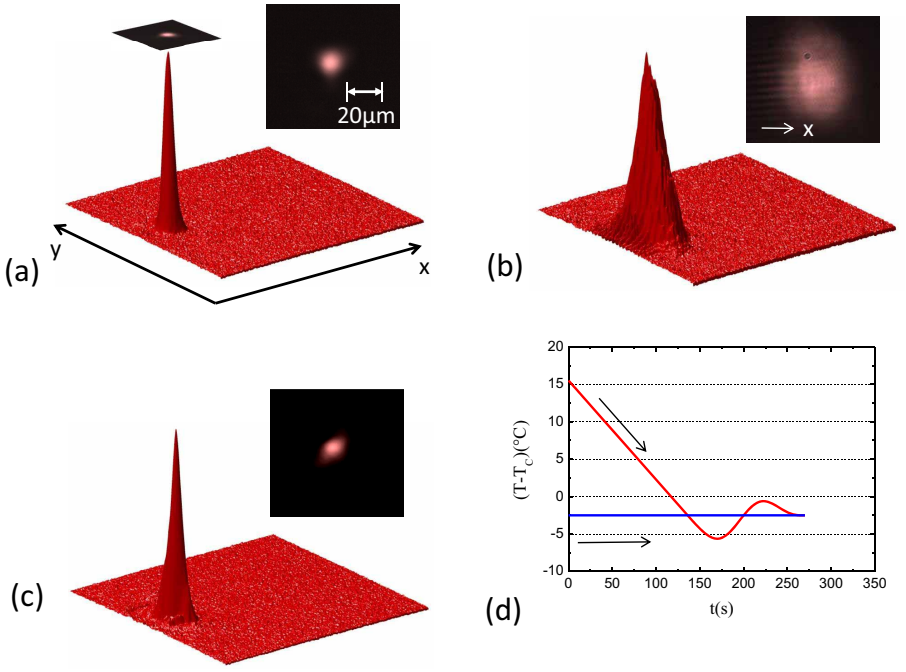

Fig. 2. Red ($\lambda = \lambda_2$) scale-free propagation and supercooling process. (a) Input intensity distribution, (b) output intensity distribution with no supercooling, (c) with the threshold supercooling α_2. (d) Comparison between the supercooling (red line) and no supercooling (blue line) glass preparation.

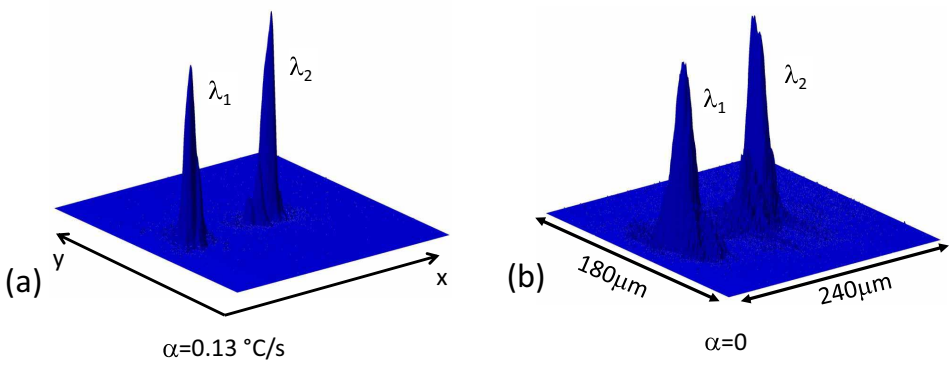

Fig. 3. Dual-wavelength beam self-trapping. (a) Output intensity distribution showing the two beams simultaneously trap to their input FWHM for $\alpha = 0.13°\mathrm{C/s}$. (b) Output diffraction intensity distribution in conditions of no supercooling ($\alpha \simeq 0$).

#154747 - $15.00 USD Received 16 Sep 2011; revised 13 Oct 2011; accepted 14 Oct 2011; published 10 Nov 2011

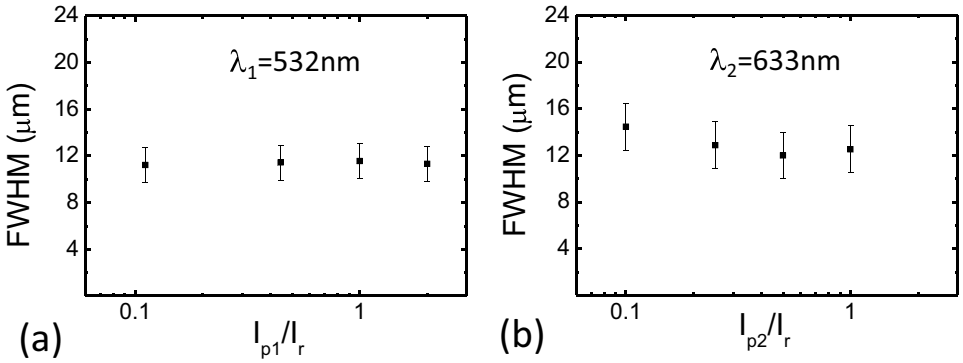

Fig. 4. Intensity-independent of the achromatic effect. The output beam FWHM is seen to be independent of the peak intensity of the two beams. The intensity can be changed independently for the two beams, the effect is unchanged from that shown in Fig. 3.

allow the imaging of the two wavelength beams simultaneously at the output. Specifically, we adopted a slanted CCD scheme, by which a slight angle between the CCD detecting surface and the direction of propagation allows both the red and green beams to be focused simultaneously.

5. Discussion

Our results have a number of interesting consequences and open the way to various developments. The first remark is that they are a quantitative validation of the scale-free model, since all previous experiments were carried out for a single wavelength. Second, they demonstrate the simple phenomenological dependence between the χ_{PNR} and the dipolar glass cooling rate, α, i.e., $L(\alpha) \propto \alpha$. Third, results indicate that scale-free optics can be implemented for wide spectral ranges, this being of utmost importance for its use in imaging and microscopy, where collected fluorescence is intrinsically non-monochormatic.

Acknowledgements

We thank G.B. Parravicini for useful discussions, and M. Deen Islam, G. Bolle, F. Mancini, and A. Spaziani for mechanical and electronics support. Research was carried out through funding from the Italian Ministry of Research (MIUR) through the ”Futuro in Ricerca” FIRB-grant PHOCOS - RBFR08E7VA and the PRIN grant n.2009P3K72Z, through European Research Council ERC grant n.201766 (COMPLEXLIGHT). Partial funding was received through the SMARTCONFOCAL and the TIRF project of the Regione Lazio (FILAS grant).

#154747 - $15.00 USD Received 16 Sep 2011; revised 13 Oct 2011; accepted 14 Oct 2011; published 10 Nov 2011